

Identification of aerodynamic sound source in the wake of a rotating circular cylinder

A. Iida¹, A. Mizuno¹ and R.J. Brown²

¹ Department of Mechanical Engineering, Kogakuin University,
 2665 Nakanomachi, Hachioji, Tokyo 192-0015, JAPAN

² School of Mechanical, Manufacturing and Medical Engineering,
 Queensland University of Technology, 2434 BRISBANE QLD 4001 AUSTRALIA

Abstract

In order to reduce aerodynamic noise radiated from the turbulent wake of bluff bodies, vorticity structures and flow field around a rotating circular cylinder at Reynolds numbers between 10^2 and 10^4 were numerically investigated. Vorticity structures and resultant aerodynamic noise is strongly dependant on the velocity ratio, which is defined as flow velocity over rotational speed to the cylinder. At low velocity ratio, the noise level and aerodynamic forces increase and an anti-symmetric vorticity structure is observed. On the other hand, the absolute value of lift-drag ratio becomes small and alternative vorticity structure disappears as the velocity ratio exceeds about 2. As a result, the fluctuating aerodynamic forces become weak and the resulting aerodynamic sound becomes small. The noise level of the rotational cylinder is 10 dB lower than that of the conventional circular cylinder. Source terms of aerodynamic sound were also visualized by using vortex sound theory. The intensity of the source term of the separated shear layer rapidly changes as the shear layers roll up. Therefore, the separated shear layers play an important role in generating aerodynamic sound at low velocity ratio. Since the anti-symmetric vorticity structure disappears at high velocity ratio, vorticity fluctuation and resultant aerodynamic noise is restrained. As a result, very interestingly, in the case of the high velocity ratio the intensity of the source term generated by the separated shear layer is maintained, however, the noise level gradually decreases. This reveals that cylinder rotation is an effective method for reducing the aerodynamic noise radiated from a turbulent wake.

Introduction

The maximum speed of high speed trains has been in an upward trend for several years [1]. Cooling flow rates inside air conditioners and computers are also increasing. Aerodynamic noise radiated from these products rapidly increases, because it is proportional to the sixth power of flow velocity. Aerodynamic noise must therefore be reduced if these products are to be further developed. Much research has been directed at noise reduction and prediction in product development. In the case of low Mach number flow, aerodynamic noise is generated by the fluctuating aerodynamic forces. Therefore aerodynamic noise from the wake of the bluff bodies depends on the large-scale eddy structures such as the Karman vorticities which cause the fluctuating lift force and flow induced vibration. In order to reduce the aerodynamic noise, control of the large vortex structures is important. It is well known that tripping wires and small holes are effective devices to reduce flow induced noise.

In this paper we discuss the effect of the rotation to reduce flow induced noise radiated from a circular cylinder in a uniform flow. In the case of potential flows, the downstream stagnation points are merged into one stagnation point when the velocity ratio of 2. Then, flow separation and vorticity structure can be controlled with the cylinder rotation. In this paper, the effect of noise reduction and vorticity break up were numerically investigated for Reynolds number between 10^2 to 10^4 at various rotational

speeds. The velocity ratio, $\alpha = u/r\omega$, defined as the ratio of the rotational speed, ω , and the uniform velocity, u , plays an important roll in noise reduction. The numerical results show the large-scale vorticities broke down at $\alpha > 2.0$ and resultant aerodynamic noise can therefore be reduced by cylinder rotation.

Numerical Methods

The governing equation used for the flow field around the rotating circular cylinder is the continuity equation and incompressible Navier-Stokes equations. The standard Smagorinsky model is adopted as the sub-grid scale model for turbulence. The Van-Dries wall-damping function is also used for modeling of near-wall effects. The Smagorinsky constant is fixed to 0.15 and the grid-filler size is computed as the cube-root of the volume of each finite element. The spatially filters of governing equations are solved by a stream-upwind, second order finite element formulation [2]. The far field sound pressure radiated from a low-Mach number flow can be calculated from Lighthill-Curle's equation [3].

$$P_a = \frac{1}{4\pi} \frac{\partial^2}{\partial x_i \partial x_j} \int_V T_{ij} \left(y, t - \frac{r}{c} \right) d^3y + \frac{1}{4\pi} \frac{\partial}{\partial x} \int_S \frac{n_i}{r} p \left(y, t - \frac{r}{c} \right) ds, \quad (1)$$

where c denotes the speed of sound, P_a is the far field sound pressure, p denotes the surface pressure. x_i and y denote the location of the observation point and coordinates at the noise source, respectively. r denotes the distance between the sound source and the observation point, n_i denotes the outward unit vector normal to the boundary surface. T_{ij} denotes the Lighthill's acoustic tensor, its contribution is negligibly small compared to that from the second term of equation at low Mach number flow. Moreover, if the body size is much smaller than the wave length of the resulting sound, equation can be written as follows;

$$P_a = \frac{1}{4\pi c} \frac{x_i}{r^2} \frac{\partial}{\partial t} \int_S n_i p \left(y, t - \frac{r}{c} \right) ds, \quad (2)$$

The surface pressure fluctuation of p is numerically estimated by using LES. The instantaneous far-field sound is obtained from equation (2). One of the authors [2] attempted to simulate the noise levels and sound spectra radiated from a turbulent wake of a circular cylinder with LES and Lighthill-Curle's acoustic analogy. The results showed that the difference between the predicted sound levels and the experimental values were within 3 dB. Moreover the predicted spectra of radiated sounds were in good agreement with those actually measured up to ten times the fundamental frequency [2]. The results showed that this method is useful for estimating aerodynamic noise level from turbulent wakes. Recent research done by Mohseni, K., Colonius, T., and Freund, J.B. [4] suggests that in some cases Lighthill's analogy may not be acceptable. But further research stills need to be done. Thus for this paper, Lighthill's analogy is adopted.

Numerical Condition

Figure 1 shows the computational mesh of the circular cylinder. The total number of three dimensional finite element meshes is about 400 thousand. At the upstream boundary of the inlet, a uniform velocity was prescribed. At the downstream boundary, the fluid traction was assumed to be zero (traction free condition). On the cylinder surface, rotational speed or non-slip condition was prescribed to simulate cylinder rotation. Symmetric boundary condition was used for both side of spanwise direction. The distance of spanwise direction is equal to 2 times the diameter.

Flow field around a rotational circular cylinder was calculated by incompressible viscous, unsteady flow simulation. To solve the fine flow structures, Large Eddy Simulation (LES) are used to simulate the unsteady turbulent flow field around a rotating circular cylinder at $Re = 10^3$ to 10^4 . Numerical simulations were carried out at the velocity ratios from 0 to 3. Aerodynamic forces, pressure fluctuation, vorticity distribution and induced noise were calculated under these conditions.

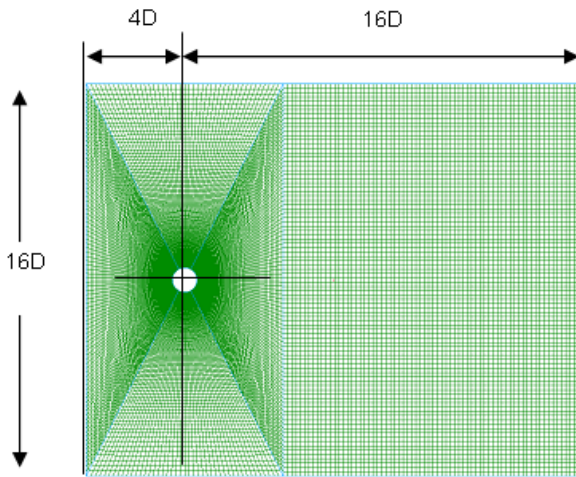


Figure 1: Computational mesh for flow around a circular cylinder.

Numerical Results

Flow Field

Figure 2 shows the separation points of the cylinder surface at $\alpha = 0.5$ and $\alpha = 2.0$. Two separation points are observed in figure 2. Since the circular cylinder is rotating counter clock wise, the bottom-side separation point S_2 moves counter clock wise. At $\alpha = 2.0$, the separation point S_2 is located near the downstream stagnation point of the stationary cylinder. As a result, the width of the wake is decreasing with the velocity ratio.

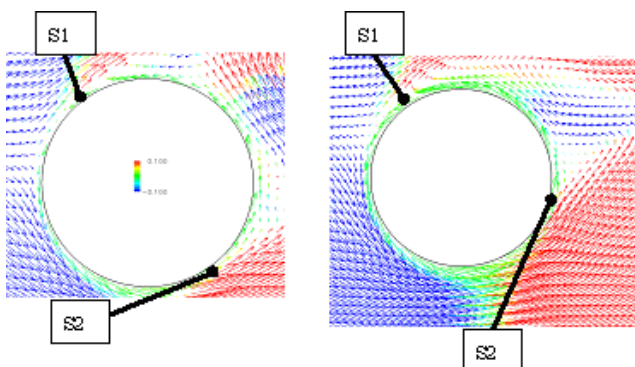


Figure 2: Separation points of a rotating cylinder at $Re=10^3$.

Figures 3 to 5 show the vorticity structures around a circular cylinder at Reynolds number of 10^3 . In the case of low velocity ratio, large-scale vorticity structures are observed and the separated shear layers roll up at just behind the cylinder. On the other hand, alternative vorticity structures disappear at the high velocity ratio. In the case of $\alpha = 3.0$, coherent structure is not observed.

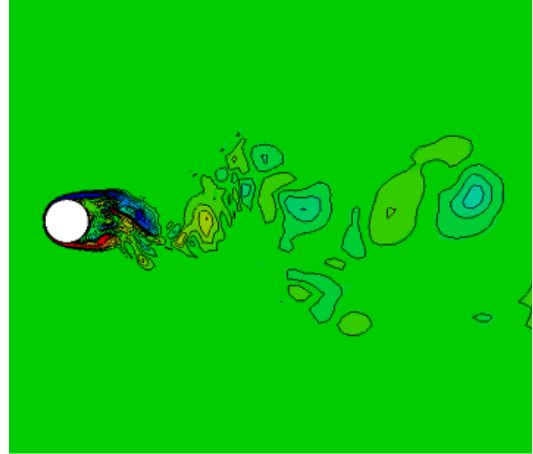


Figure 3: Contours of vorticity around a rotating cylinder at $Re=10^3$, $\alpha = 0.0$.

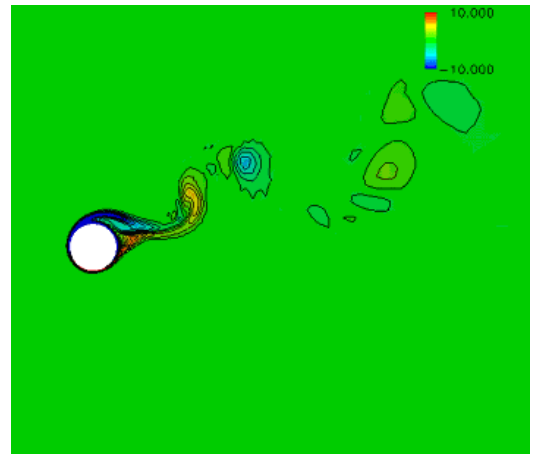


Figure 4: Contours of vorticity around a rotating cylinder at $Re=10^3$, $\alpha = 2.0$.

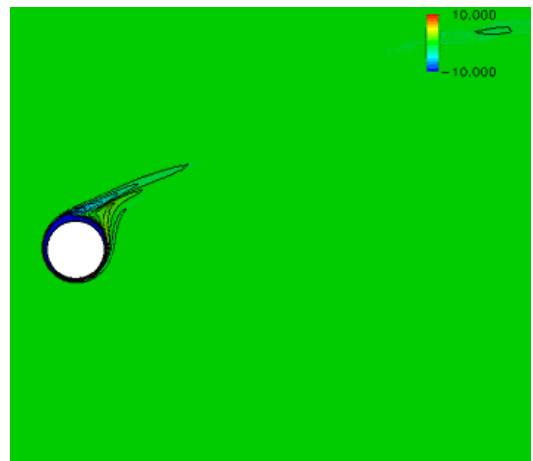


Figure 5: Contours of vorticity around a rotating cylinder at $Re=10^3$, $\alpha = 3.0$.

The aerodynamic forces strongly depend on the vorticity structures as shown in Figure 6. The ratio of lift and drag forces increases with the velocity ratio up to $\alpha = 2.0$. This corresponds to the velocity ratio of the upper limit of the large-scale structure in existence. The ratio of lift and drag forces decrease over $\alpha = 2.0$. This tendency is almost equal to numerical results with the vortex method [5]. In the case of the high velocity ratio, lifting force decreases because the large scale vorticity disappeared. However, friction drags of the cylinder surface increase with the speed of rotation. Therefore, the lift and drag ratio is decreases at high velocity ratio and the fluctuating lifting force also decreases.

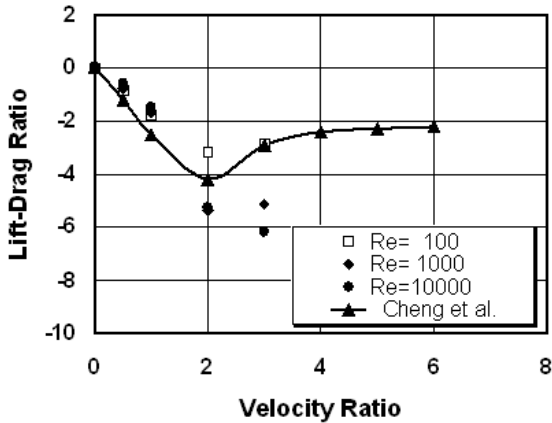


Figure 6: Lift-drag ratio of a rotating circular cylinder.

Aerodynamic Noise

Figure 7 shows the aerodynamic noise from a rotating circular cylinder. The far-field noise is calculated from equation (2). These simulations are carried out under the compact body assumption, the refraction and reflection is neglected. The predicted noise level does not depend on the Reynolds number, but strongly depends on the velocity ratio of the cylinder rotation. When the alternative vorticity structures exist, noise levels increase in comparison to noise level of non-rotating cylinder. On the other hand, sound levels decrease at high velocity ratio of $\alpha > 2.0$. The aerodynamic noise from a rotational circular cylinder at $\alpha = 3.0$ is 10dB lower than that of the stationary circular cylinder. It revealed that the rotational speed is one of the control factors of aerodynamic noise reduction.

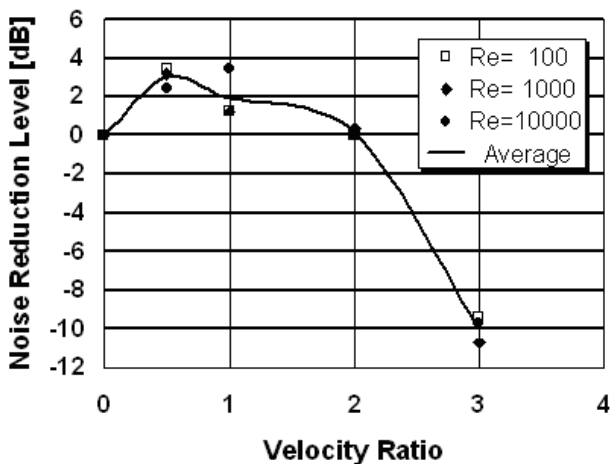


Figure 7: Noise reduction effect on velocity ratio of a rotating circular cylinder.

Noise Source Identification

Figures 8 to 10 are aerodynamic noise source term calculated by the Powell's theory [6]. The Lighthill-Curle's theory is useful to estimate the aerodynamic noise; however the Lighthill-Curle's theory gives us no information about the relationship between unsteady vorticity fluctuation and aerodynamic sound. In order to control the aerodynamic sound generation, vorticity contribution of sound generation is important to formulate an algorithm of noise control. The Powell's vortex sound theory directly reflects the aerodynamic aspects of the aerodynamic sound generation. Aerodynamic sound can be written as follows:

$$\left(\frac{1}{c_0} \frac{\partial^2}{\partial t^2} - \nabla^2\right) P_a = \rho_0 \text{div}(\boldsymbol{\omega} \times \boldsymbol{v}). \quad (3)$$

The above equation shows that the aerodynamic noise is calculated by using the wave equation with a source term of $\rho_0 \text{div}(\boldsymbol{\omega} \times \boldsymbol{v})$. Figures 8 and 10 show the source term of the rotating circular cylinder. In the case of non-rotating cylinder, the aerodynamic sound source lies the just behind the cylinder. It is remarkable that the aerodynamic sound source is concentrated in a small region. In this region, the alternating vortices come from both sides of the cylinder, and the separated shear layer is stretched by this vortex motion. The separated shear layer therefore rolls up at this region.

In case of $\alpha = 2.0$, the source term declines due to the effect of the rotation, however, the distribution of the source term is almost the same as $\alpha = 0.0$. Then noise level of $\alpha = 2.0$ is almost same as the noise of $\alpha = 0.0$. In contrast, distribution of a sound source is different in the case of $\alpha = 3.0$. The sound source only exists and around the cylinder surface and source term is not seen in the wake of the cylinder.

Figure 11 shows the iso-surface of sound source term of the circular cylinder. The iso-surface has three-dimensional complicated structure at $\alpha = 0.0$. Because the structure of the wake is unstable, the sound source changes in time domain. If the source term has a high velocity ratio, the sound source term has two-dimensional structure as shown in Figure 11 (b). Then noise source fluctuation is not so large. The generated sound is therefore small in the case of $\alpha = 3.0$.

The origin of the aerodynamic source comes from the separated shear layers, because the velocity gradient is large at the boundary layer of the cylinder surface. In the case of rotating cylinder, velocity gradient is large compared with the stationary cylinder. The intensity of the source term due to the separated shear layer is large at the high velocity ratio; however, aerodynamic sound is small at the high velocity ratio. Since the aerodynamic noise is caused by the unsteady vortex motion, the aerodynamic sound generation depends on not only on the source term intensity of shear layers but also in the source term fluctuation in time and spatial domains. It is revealed that the vorticity stretching and roll up is important to generate aerodynamic sound.

Conclusions

Vorticity structures and flow field around a rotating circular cylinder at Reynolds numbers between 10^2 and 10^4 were numerically investigated. The fluctuating aerodynamic becomes weak and the resulting aerodynamic sound becomes small. The noise level of the rotational cylinder is 10 dB lower than that of the non-rotating cylinder. Aerodynamic sound source terms were numerically visualized by using Powell's theory. The result of the sound source identification shows the aerodynamic sound generated at the formation region of Karman vorticities.

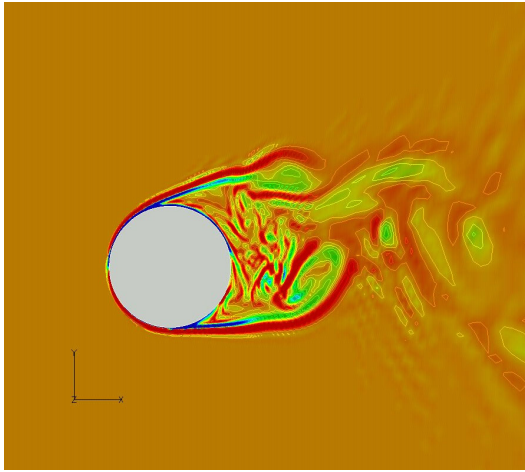


Figure 8: Distribution of aerodynamic sound source term around a rotating circular cylinder at $\alpha = 0.0$.

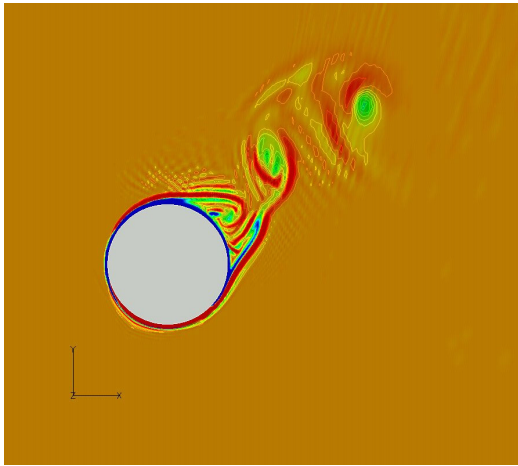


Figure 9: Distribution of aerodynamic sound source term around a rotating circular cylinder at $\alpha = 2.0$.

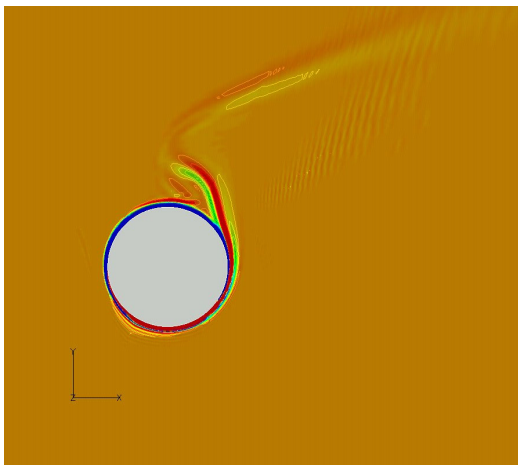
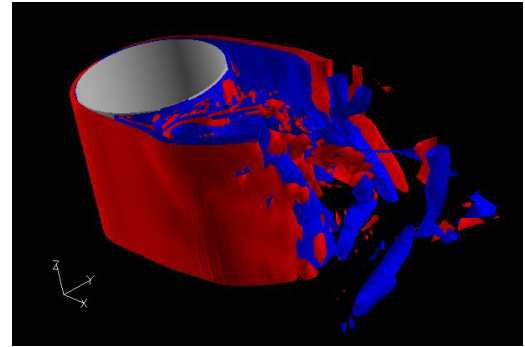
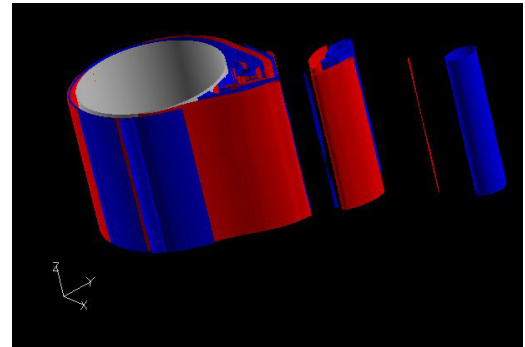


Figure 10: Distribution of aerodynamic sound source term around a rotating circular cylinder at $\alpha = 3.0$.



(a) $\alpha = 0.0$



(b) $\alpha = 2.0$

Figure 11: Iso-surface of aerodynamic sound source term around a rotating circular cylinder at $Re = 10^3$.

Therefore, the separated shear layers play an important role in generating aerodynamic sound at low velocity ratio. Since the aerodynamic noise is caused by the unsteady vortex motion, the aerodynamic sound generation depends on not only source term intensity of the shear layers but also the source term fluctuation in time and spatial domains. The resultant aerodynamic noise is therefore restrained at high velocity ratio. It reveals that cylinder rotation is an effective method to reduce the aerodynamic noise radiated from a turbulent wake.

Acknowledgements

The authors thank Professor Chisachi Kato, Institute of Industrial Science, University of Tokyo for his many fruitful discussions on the generation mechanism of aerodynamic sound and technical advice on numerical simulations.

References

- [1] King III, W. F., A Precip of Development in the Aeroacoustics of Fast Trains, *J. Sound Vibration*, **193**(1), 1996, 349-358.
- [2] G Kato, C., *et al.*, Numerical Prediction of Aerodynamic Sound by Large Eddy Simulation, *Trans. Jpn. Soc. Mech. Eng.* (in Japanese), **Vol. 60** No.569, **B**, 1994, 126-132.
- [3] Curle, N., The Influence of Solid Boundaries upon Aerodynamic Sound, *Proc. Roy. Soc. London*, **A231**, 1955, 505-514.
- [4] Mohseni, K., Colonius, T., and Freund, J.B., An evaluation of linear instability waves as sources of sound in a supersonic turbulent jet, *Physics of Fluids.*, **14**(10), 2002, 3593-3600
- [5] M. Cheng, Y. T. Chew and S.C. Luo., Numerical simulation of Rotational Circular Cylinder, *Finite Elements in Analysis and Design*, **Vol.18**, 1994, 225-236
- [6] Powell, A., Theory of vortex sound, *J. Acoustical Society of America*, **36**, 1964, 177-195